

Provided for non-commercial research and education use.  
Not for reproduction, distribution or commercial use.



This article appeared in a journal published by Elsevier. The attached copy is furnished to the author for internal non-commercial research and education use, including for instruction at the authors institution and sharing with colleagues.

Other uses, including reproduction and distribution, or selling or licensing copies, or posting to personal, institutional or third party websites are prohibited.

In most cases authors are permitted to post their version of the article (e.g. in Word or Tex form) to their personal website or institutional repository. Authors requiring further information regarding Elsevier's archiving and manuscript policies are encouraged to visit:

<http://www.elsevier.com/authorsrights>



Contents lists available at ScienceDirect

## Comparative Biochemistry and Physiology, Part B

journal homepage: [www.elsevier.com/locate/cbpb](http://www.elsevier.com/locate/cbpb)

## Characterisation and expression of the biomineralising gene *Lustrin A* during shell formation of the European abalone *Haliotis tuberculata*



B. Gaume<sup>a,\*</sup>, F. Denis<sup>a,b</sup>, A. Van Wormhoudt<sup>a</sup>, S. Huchette<sup>c</sup>, D.J. Jackson<sup>d</sup>,  
S. Avignon<sup>a</sup>, S. Auzoux-Bordenave<sup>a,e</sup>

<sup>a</sup> UMR BOREA (Biologie des Organismes et Écosystèmes Aquatiques), MNHN/CNRS 7208/IRD 207/UPMC, Muséum national d'Histoire naturelle, Station de Biologie Marine de Concarneau, 29900 Concarneau, France

<sup>b</sup> Université du Maine, 72085 Le Mans, France

<sup>c</sup> Ecloserie France-Haliotis, Kerazan, 29880 Plouguerneau, France

<sup>d</sup> University of Göttingen, Courant Research Centre Geobiology, 37077 Göttingen, Germany

<sup>e</sup> Université Pierre et Marie Curie, Paris VI, 75005 Paris, France

## ARTICLE INFO

## Article history:

Received 21 October 2013

Received in revised form 29 November 2013

Accepted 30 November 2013

Available online 7 December 2013

## Keywords:

Biomineralisation

*Haliotis tuberculata*

Larval development

*Lustrin A*

Shell

## ABSTRACT

The molluscan shell is a remarkable product of a highly coordinated biomineralisation process, and is composed of calcium carbonate most commonly in the form of calcite or aragonite. The exceptional mechanical properties of this biomaterial are imparted by the embedded organic matrix which is secreted by the underlying mantle tissue. While many shell-matrix proteins have already been identified within adult molluscan shell, their presence and role in the early developmental stages of larval shell formation are not well understood. In the European abalone *Haliotis tuberculata*, the shell first forms in the early trochophore larva and develops into a mineralised protoconch in the veliger. Following metamorphosis, the juvenile shell rapidly changes as it becomes flattened and develops a more complex crystallographic profile including an external granular layer and an internal nacreous layer. Amongst the matrix proteins involved in abalone shell formation, *Lustrin A* is thought to participate in the formation of the nacreous layer. Here we have identified a partial cDNA coding for the *Lustrin A* gene in *H. tuberculata* and have analysed its spatial and temporal expression during abalone development. RT-PCR experiments indicate that *Lustrin A* is first expressed in juvenile (post-metamorphosis) stages, suggesting that *Lustrin A* is a component of the juvenile shell, but not of the larval shell. We also detect *Lustrin A* mRNAs in non-nacre forming cells at the distal-most edge of the juvenile mantle as well as in the nacre-forming region of the mantle. *Lustrin A* was also expressed in 7-day-old post-larvae, prior to the formation of nacre. These results suggest that *Lustrin A* plays multiple roles in the shell-forming process and further highlight the dynamic ontogenic nature of molluscan shell formation.

© 2013 Elsevier Inc. All rights reserved.

### 1. Introduction

Biomineralisation is the process by which living organisms deposit and elaborate minerals, often with exceptional mechanical properties (see Mann, 2001; Weiner and Dove, 2003 for review). An ability to biomineralise has made the Mollusca one of the most successful invertebrate phyla and has supported their colonization of terrestrial, freshwater and marine environments. Although the shape and crystallographic microstructure of the molluscan shell are highly diverse, this biomineral

is lost often constructed from calcium carbonate ( $\text{CaCO}_3$ ) primarily as calcite and/or aragonite depending on species, with vaterite and amorphous ( $\text{CaCO}_3$ ) phases also occurring (Lowenstam and Weiner, 1989; Addadi et al., 2003).

The abalone shell has long been used as a model to study the basic mechanisms of gastropod shell formation. This is because its highly ordered columnar and lustrous nacre imparts an aesthetic quality to the material that is of value to industries such as gemmology and biomimetics. Shell formation is achieved by the underlying mantle, a thin sheet of tissue that overlies the dorsal surface of the abalone. The distal-most edge of the mantle is divided into two folds separated by the periostracal groove—an “outer” dorsal-most fold, and an “inner” ventral-most fold (Sud et al., 2002). From the periostracal groove and the outer mantle fold, an organic matrix composed of proteins, polysaccharides and lipids is secreted. With precise control, this organic matrix governs the nucleation, growth, orientation and inhibition of  $\text{CaCO}_3$  crystal depositions (Falini et al., 1996; Mann, 2001). The characteristics

\* Corresponding author at: Laboratoire de Biologie Marine, DYNECAR EA 926, Université des Antilles et de la Guyane, Campus de Fouillole, 97110 Pointe-à-Pitre, Guadeloupe. Tel.: +33 690982897.

E-mail addresses: [beatrice-gaume@hotmail.fr](mailto:beatrice-gaume@hotmail.fr) (B. Gaume), [fdenis@mnhn.fr](mailto:fdenis@mnhn.fr) (F. Denis), [avw@mnhn.fr](mailto:avw@mnhn.fr) (A. Van Wormhoudt), [sylvain.huchette@wanadoo.fr](mailto:sylvain.huchette@wanadoo.fr) (S. Huchette), [djackson@uni-goettingen.de](mailto:djackson@uni-goettingen.de) (D.J. Jackson), [bordenav@mnhn.fr](mailto:bordenav@mnhn.fr) (S. Auzoux-Bordenave).

and composition of the organic matrix define the specific mineralogy and microstructure of individual shell layers (Addadi and Weiner, 1985). In gastropods and particularly in abalone, functional regionalisation of the mantle can be recognised by distinct fields of shell-forming gene expression (Jackson et al., 2006).

A major challenge that occupies the field of biomineralisation is to both identify and characterise the function of individual matrix protein. Transcriptomic and proteomic analyses have led to the identification of many novel shell-forming gene sequences, with the majority identified in bivalves (Jackson et al., 2006; Marin et al., 2008; Joubert et al., 2010). In contrast, less than 20 proteins have been identified using proteomic approaches in the Haliotidae: Lustrin A (Shen et al., 1997), AP7 and AP24 in *Haliotis rufescens* (Michenfelder et al., 2003), perlucin, perlustrin (Weiss et al., 2000), perlwapin (Treccani et al., 2006), and perlinhibin (Mann et al., 2007) in *Haliotis laevigata*, and 12 proteins recently identified in *Haliotis asinina* (Marie et al., 2010). All of these proteins were isolated from the adult abalone shell, and some studies have demonstrated their role in the biomineralisation process in vitro (Blank et al., 2003; Wustman et al., 2003, 2004; Treccani et al., 2006; Mann et al., 2007; Amos and Evans, 2009). Lustrin A was the first protein to be isolated from the nacreous material of the red abalone shell (Shen et al., 1997). Amongst other functions, this protein is believed to act as a 'molecular shock absorbing CaCO<sub>3</sub>-adhesive' (Smith et al., 1999). This is primarily due to its repetitive-domain sequence architecture and the presence of a large domain of glycine and serine residues and Cys-rich domains. It may also possess protease inhibitor properties due to the presence of a C-terminal domain with sequence homology to the Whey Acidic Proteins (Shen et al., 1997). However these putative functions are yet to be experimentally validated.

What has received far less attention is the shell-forming process during abalone development. Many biomineralisation studies are primarily focused on the biomineral from a single time point (typically the final adult shell), and the ontogenic changes that culminate in the production of an adult mollusc shell are overlooked. It is known that significant morphological, microstructural and mineralogical changes take place in the shell from the first signs of biomineralisation in the larvae through metamorphosis and juvenile growth to production of the mature adult shell (Courtois de Viçose et al., 2007; Jackson et al., 2007; Jardillier et al., 2008; Auzoux-Bordenave et al., 2010). Despite these dramatic ontogenic shifts in relation to shell formation, the molecular mechanisms underlying these processes remain largely unknown.

In the European abalone *Haliotis tuberculata*, the first mineralized shell, protoconch I, is secreted by the shell field in trochophore stages (19 h post-fertilisation, hpf). The veliger larva (25 hpf) displays a round shell, protoconch II, which surrounds the soft body. At this stage, the mantle begins to differentiate in the dorsal part of the larva. Following metamorphosis (5–6 days) the flattened shell of the juvenile is elaborated, and begins to attain pigment and ornamentation to finally give rise to the adult shell (Gaume et al., 2011). The occurrence of the first nacre tablets was observed in two-month old juvenile abalone (Auzoux-Bordenave et al., 2010). We recently demonstrated a correlation between the main phases of abalone shell formation and the enzymatic activities of both carbonic anhydrase and alkaline phosphatase (Gaume et al., 2011). Furthermore, two genes encoding carbonic anhydrases have been characterised from the shell-forming mantle tissue of *H. tuberculata* (Le Roy et al., 2012). In another recent work, partial protein sequences isolated from the shell matrix of the European abalone were found to match with EST sequences acquired from *H. asinina* mantle tissue (Bédouet et al., 2012).

To further our understanding of the ontogenic process of shell and nacre formation in *H. tuberculata*, we have isolated and characterised the expression of the putative nacre-forming gene *Lustrin A*. This study highlights some of the dynamic molecular activity that underlies early juvenile shell formation in *H. tuberculata*, and indicates that *Lustrin A* likely plays a role in processes other than nacre deposition.

## 2. Material and methods

### 2.1. Animals

*H. tuberculata* larvae, juveniles and adults were collected at the hatchery France-Haliotis (S. Huchette, Plouguerneau, France). Larval stages (7, 17, 22, 41, 65 and 90 hpf) were obtained from a controlled fertilisation conducted in July 2010 in a water temperature of 16 °C ± 0.5 °C. Fresh, living larvae, (around 5000 per stage) were filtered on a 40-µm-sieve and immediately stored in liquid nitrogen or fixative according to the experiments. Post-larvae (7-day-old) and juveniles (2-month- and 1-year-old), grown on plates covered with micro-algae, were detached with a pipet and sampled in 15 mL tubes for further analysis. Adult abalones (3-year-old) were maintained in an 80 L-tank supplied with aerated natural seawater. Natural salinity and photoperiod were kept constant. Abalones were fed once a week with the red algae *Palmaria palmata*. Two days before sampling adult material, the algae were removed and inflow seawater was UV treated to minimise bacterial contamination.

### 2.2. Total RNA extraction

For RNA extractions, larvae and juveniles were frozen in liquid nitrogen at the hatchery. Adult mantle tissue was collected by dissection under sterile conditions and immediately incubated in Trizol solution (Invitrogen). Around 1000 larvae of each developmental stage, whole juveniles and 200 mg of adult tissues were incubated with 1 mL of Trizol and manually ground in a 1.5 mL tube. Total RNA was extracted according to the manufacturer's instructions. RNA was treated with Deoxyribonuclease I amplification Grade (Sigma) to eliminate genomic DNA.

### 2.3. Northern blot

Five microgram of adult *H. tuberculata* total mantle RNA was resolved on a 1.2% denaturing MOPS agarose formaldehyde gel. Following electrophoresis, the RNA was transferred overnight by downward capillary to a charged Nylon membrane. RNA was then cross-linked to the membrane by exposure to UV light for 2 min. The membrane was then pre-hybridised for 2 h in hybridisation buffer (5× SSC; 5 mM EDTA; 50% formamide; 100 µg·mL<sup>-1</sup> Heparin; 0.1% Tween20; 1× Denhardt's solution; 100 µg·mL<sup>-1</sup> sonicated salmon sperm) in a hybridisation oven at 60 °C. Following pre-hybridisation, an 887 bp DIG labelled probe derived from *H. asinina* *Lustrin* with 94% homology to the *H. tuberculata* sequence was applied at 400 ng·mL<sup>-1</sup> in hybridisation buffer. Hybridisation was allowed to proceed overnight at 60 °C. Three 15 min-washes were performed at 60 °C using a solution of 1% SDS and 0.1× SSC. The membrane was then thoroughly rinsed in sterile H<sub>2</sub>O to remove residual SDS and was equilibrated for 15 min in MAB (0.1 M maleic acid; 0.15 M NaCl). Five millilitre of a 2% blocking solution was then applied (2% w/v blocking powder from Roche in MAB) and incubated for 30 min at room temperature. One microliter of Roche's anti-Digoxigenin-AP Fab fragments conjugated to alkaline phosphatase was then added to the blocking solution and incubated with gentle agitation for 30 min at room temperature. Membrane was then washed several times with MAB + 0.1% Tween20 and equilibrated for 5 min in colour detection buffer (0.1 M Tris pH 9.5; 0.1 M NaCl). Colour substrate solution (detection buffer; 225 µg·mL<sup>-1</sup> NBT; 175 µg·mL<sup>-1</sup> BCIP) was then applied to the membrane and the colour reaction monitored. Colour development was terminated by washing the membrane in water.

### 2.4. cDNA synthesis, RACE PCR, cloning and sequencing

Reverse transcription was carried out using 400 units of SuperScript III Reverse Transcriptase (Invitrogen) on 1 µg of total RNA and an

**Table 1**  
Primers used in this study.

Primer		Sequence (5' > 3')	Amplicon length (bp)	Purpose
Ht-Lus-degF	Forward	TGGTGYTNTAYAAAYTTYGYCC		
Ht-Lus-degR	Reverse	RCARTCRTRTRCRAARCA	339	<i>Lustrin A</i> identification
GSP	Forward	GTCCGGCAGTTCCTACTGT	480	3'-RACE
Crev	Reverse	GGCCCTCGTTTGAGATATCT		5'-RACE
Ofw	Forward	GGATGAATACGGGTATGCTGT		
Frev	Reverse	TGACACAGGTAGGAAGTCC	980	5'-RACE
DFw	Forward	GTTCTCTACACCATCTGG		
ACrev	Reverse	TCAAAGCATGGCTTTTGACA	356	5'-RACE
Ht-LusFw	Forward	TCTGTCCGGCAGTTCCTAC		
Ht-LusR	Reverse	CTGGGGCACTGTAAGTTGGT	127	Gene expression (RT-PCR)
Ht-ActF	Forward	CCATCTACGAGGGATATGCC		
Ht-ActR	Reverse	CAATCCAGACGGAGTATTCC	534	Gene expression (RT-PCR)

oligo(dT)<sub>15</sub> primer (Promega) according to the supplier's instructions. To identify *Lustrin A* in *H. tuberculata*, PCR amplification was initially performed using degenerate primers *Ht-Lus-degF* and *Ht-Lus-degR* (see Table 1 for all primer sequences). These primers were designed to bind to the carboxyl-most Cys-rich domain and the basic domain of *H. rufescens* *Lustrin*. Platinum Taq DNA polymerase (Invitrogen) was used for PCR amplification with a hybridisation temperature of 51 °C. The resulting 339 bp PCR product was cloned into pGEM-T easy vector system II (Promega). Competent *Escherichia coli* (JM109, Promega) were transformed and plated out on LB/Agar/Ampicillin (100 µg·mL<sup>-1</sup>) plates with X-gal and IPTG for blue/white screening. Colonies were screened by PCR and Standard Sanger DNA sequencing of three independent clones was performed using M13 primers. Sequencing reactions were carried out using BigDye Terminator v3.1 (Applied Biosystems). Thermocycling was as follows: initial denaturation for 2 min at 96 °C, then 40 cycles of 30 s at 96 °C, 30 s at 50 °C and 4 min at 60 °C in an automatic sequencer Applied Biosystems/Hitachi (model 3130). To obtain the 5' and 3' ends of *Ht-Lus*, rapid amplification of cDNA ends (RACE) was performed with a 3'/5'-RACE kit (Boehringer Mannheim). 3'-RACE amplification of cDNA was performed using the oligo dT anchor primer and the gene specific primer (GSP). 5'-RACE was done using firstly Crev and oligodT anchor after dA tailing of the cDNA, then Frev and anchor as the second round of PCR. Each fragment obtained was cloned in pGEM-T easy vector system II easy vector and sequenced as described above. To obtain the complete sequence from the same individual, two PCR reactions were performed; the first one with OFw and Frev as primers, including the first part of the cDNA, the second one with Dfw and ACrev.

### 2.5. Reverse transcriptase PCR (RT-PCR)

To investigate the expression of *Ht-Lus* during the development of *H. tuberculata*, RT-PCR was performed using platinum Taq DNA polymerase (Invitrogen) and specific primers designed to the last carboxyl-most Cys-rich domain (*Ht-LusFw* and *Ht-LusR*; Table 1) generating a 127 bp amplification product. A PCR control was also performed with the reference gene *actin* with the specific *H. tuberculata* primers *Ht-ActF* and *Ht-ActR* (Table 1). This control ensured equal cDNA synthesis efficiency across samples, and equal loading into the RT-PCR reaction. All PCR reactions were cycled for 35 cycles and PCR products were resolved on a 2% agarose gel.

### 2.6. Whole mount in situ hybridisation (WMISH)

For WMISH, live abalone larvae and juveniles were relaxed in 0.6 M MgCl<sub>2</sub> (diluted in PBS-Tween 3% NaCl, pH 7.4) for 10 to 20 min prior to fixation. Animals were then fixed in 4% paraformaldehyde (diluted in PBS-Tween 3% NaCl, pH 7.4) for 1 h at room temperature. After three rinsing in PBS-Tween 0.1%, larvae and juveniles were stored at -20 °C in 100% ethanol. *Ht-Lus* fragment of 339 bp was used to generate a digoxigenin-labelled riboprobe. A PCR product produced using M13

primers and the cloned *Ht-Lus* fragment as a template was purified using a Qiagen column. This purified DNA was used as a template for SP6 and T7 RNA polymerases in order to synthesize sense and anti-sense DIG labelled probes according the manufacturer's instructions provided by Roche.

Prior to WMISH, larvae and juveniles were rehydrated, and then decalcified for 30–40 min in 100 and 350 mM EDTA respectively. The remaining periostracum was manually removed from juveniles with forceps. Whole mount in situ hybridisation and antibody detection were performed following previously described protocols (Giusti et al., 2000; Jackson et al., 2006).

## 3. Results

### 3.1. Isolation and characterization of the primary *Lustrin A* sequence from *H. tuberculata*

Degenerate *Lustrin A* primers on *H. tuberculata* produced a sequence of 339 bp. A BLASTx search against GenBank nr confirmed that this sequence corresponded to *Lustrin A*. 3' and 5'-RACE experiments generated a sequence of 1436 bp with an open reading frame of 1339 bp which appears to be the 3' end of the transcript (Fig. 1). We have named the *H. tuberculata* *Lustrin A* sequence *Ht-Lus* and the nucleotide sequence is available from GenBank with the accession number HM852427.

The deduced amino acid sequence of *Ht-Lus* (Fig. 1) displays a similar modular arrangement to *Lustrin A* from *H. rufescens* (Shen et al., 1997) (Fig. 2). Using that nomenclature, the sequence of the Pro-rich domain in *Ht-Lus* contains 8 Pro and presents 27% of identity with P5 domain in *H. rufescens* (Fig. 1). The partial sequence of *Ht-Lus* contains two Cys-rich domains of 79 residues each. These Cys-rich domains begin with a Asp-Pro-Cys motif and end with two Cys residues as is the case in all Cys-rich domains in *H. rufescens*. The first Cys-rich domain in *Ht-Lus* shares 69% identity with C7 domain in *H. rufescens*. The second Cys-rich domain in *Ht-Lus* follows the Gly-Ser-rich domain and shows 81% of identity with C10 domain in *H. rufescens*. These two domains are connected by a Gly-Ser-rich domain of 153 amino acids including 136 Gly/Ser residues. The Gly-Ser-rich domain in *Ht-Lus* is 119 residues smaller than that in *Ht-Lus* (Fig. 2). The predicted pI (11.80) of the basic domain of *Ht-Lus* (which follows the C10 domain) is very slightly more basic than that in *H. rufescens* (11.74). The C-terminus domain of *Ht-Lus* is 43 residues long and exhibits strong sequence similarity with several protease inhibitors as is the case in *H. rufescens*. This domain exhibits 86% identity with the Whey Acidic Protein (WAP) domain in *H. rufescens* *Lustrin A*. The eight cysteine residues, known to form four-disulphide bonds in WAPs, are located in conserved positions in both abalone species.

Our northern blot results indicate that there are 2 *Lustrin* transcripts present in the adult mantle tissue of *H. tuberculata* (Fig. 3). These are significantly larger than the two presumably homologous transcripts reported by Shen et al. (1997) for *H. rufescens* (6.4 and 6.0 kb for *H. tuberculata* vs. 5.5 and 4.7 kb for *H. rufescens*).

```

1 GGATGAATACGCGGTATGCTGTTTGTAGTTCTGTTCAGTTCCACCAACACCTGGGCCAAC 60
1 D E Y A V C C F S S V P V P P T P G P T 20
61 TTTACCGTCACCAGGAAGACCAACACCGGGGATCCCTGTGCACCTGGTGTAAATGTGAA 120
21 L P S P G R P N T G D P C A P G V N V N 40
121 CTGTAACAAGAGGCGAGTGCAGACTGGTAGCTGACTGTGACCGATGGCCGTGTTATGCGCG 180
41 C T R G E C R L V A D C D R W P C Y A R 60
181 TCCAGCGTGTGTTGATCCATCTCCAACACCATCAGTTCAGTGTCCCTGTGGAAAGCCTGC 240
61 P A C V D P S P T P S V Q C P V G K P A 80
241 GCTTAATGGCTCTCTACTTGAATCTCATGTAGAGAGAGGGATACATGCCCTTGAATAC 300
81 L N G S L L E I S C R E R D T C P L N T 100
301 TCGGTGTTATAACGAAGCTGTCTGTGTATCCGAGTACCAGGAATCAACCACAGGTTTC 360
101 R C Y N E A V C C I R V P G I N P P G S 120
361 AGGTC AAGCTCAGGCTCAGGCTCAGGCTCAGGATCAGGATCAGCTTGTAGTTTC 420
121 G S S S G S G S G S G S G S G S G S A L S S 140
421 AGGATCAGGCCACAGTTCAGGCTCAGGCTCCAGTTC AAGATCAGGCTCTGGATCAGGCTC 480
141 G S G P S S G S G S S R S G S G S G S 160
481 CAGTTCAGGATCAGGCTCTGGCTTAAGTTCAGGATCAGGCTCCAGTTCAGGATCAGGCTC 540
161 S S G S G S G L S S G S G S G S G S G S 180
541 TGGCTCAGTTCAGGATCAGGCTCCAGTTCAGGCTCAGGCTCCAGTTCAGGATCAGGCC 600
181 G F S S G S G S S S G S G S S S G S G P 200
601 CAGTTCAGGCTCAGGCTCCAGTTCAGGATCAGGCTCCAGTTCAGGCTCAGGCTCCAGTTC 660
201 S S G S G S S S G S G S S S G S G S S S 220
661 AGGCTCAGGCTCCAGTTCAGGATCAGGCCCTCTCATCAGGCTCTGGCTTTCAGTTCAGG 720
221 G S G S S S G S G P S S S G S G F S S G 240
721 ATCAAGTTC AAGCTCAGGCTCAGACCAGACTCAGACTACTTCTCAAGTTCAGTGTCAA 780
241 S S S S G S D R D S D Y F S S S L S N 260
781 CTCAGTTCAGGTC CGGATCGGGATCAGGAAGGAAATGGAGCAAGTATGACACTGA 840
261 S G S G S G S G S G R S N G A S Y D T D 280
841 TTCAGGCTCAGATGGCCCCCTGGCGACCTGCCGCAAGACCCTTGTACTCCCGGGCTGA 900
281 S G S D G P P F G D L P Q D P C T P G L N 300
901 TATCAACTGCACAGAAGTGTGTTGCCGACTATTAGCCTGGTGTGTTGTACAGCATCTGTC 960
301 I N C T E G V C R L L A W C L Y S I C P 320
961 GGCAGTTCCTACCTGTGTGTCAGCCGTTCTCTACACCATCTGGGAGTTGTCCAGTTAGCCT 1020
321 A V P T C V S R S P T P S G S C P V S L 340
1021 GCCAGCCCTGAAC TACTTGGTAACGAGGTATCCTGCAGAACCAACTTACAGTGC C C C C 1080
341 P A L N Y F G N E V S C R T N L Q C P S 360
1081 TAACACCTACTGTACAAGCCCTGGGATCTGTTGCTACCGAGGACCGAAAGCTGATCGTCG 1140
361 N T Y C T S P G I C C Y R G P K A D R R 380
1141 AAGTTTGTAGATACTGGAGAAGATATCTCAAACGAGGGCCCTCAGGCAACGTATCGGAAA 1200
381 S F R Y W R R Y L K R G P S G K R I G K 400
1201 GCCCGGAAGTTGCCCCCGCTAAGGCCAGGATGGGCTGGCGCCTGTGTTGAGGAGTGT 1260
401 E G S C P A V R P G W A G A C V E E C F 420
1261 CTGTGACAACGACTGCAGAGGGAATCTGAAATGTTGAGCAATGGGTGTGGACATACTTG 1320
421 C D N D C R G N L K C C S N G C G H T C 440
1321 TCAAAAGCCATGCTTGAATAACAACCTGCACAAACGTTTATTTATAGCTATCTACATTA 1380
441 Q K P C F E * 446
1381 TCAAAATATAAGCACTTATGTTTGTAAAAA AAAAAAAAAAAAAAAAAAAAAAAAAAAAA 1436
    
```

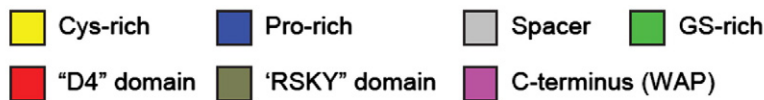


Fig. 1. Partial nucleotide and deduced amino acid sequence of Lustrin A (*Ht-Lus*) from the mantle of the European abalone *Haliotis tuberculata* (GenBank accession no HM852427). The different domains of Lustrin A as described by Shen et al. (1997) and Wustman et al. (2003) are colour coded. Degenerate primers used to isolate an initial fragment of *Ht-Lus* are underlined. An asterisk represents the terminal codon.

3.2. Expression of *Ht-Lus* during abalone development

The expression of *Ht-Lus* was analysed by RT-PCR in different developmental stages of *H. tuberculata* including larvae, juveniles and adult mantle tissue (Fig. 4). During embryonic and planktonic larval stages (eggs, trochophore and veliger larvae), *Ht-Lus* transcripts were either extremely rare or not present at all (Fig. 4). Following metamorphosis,

2-month-old and 1-year-old juveniles express *Ht-Lus* (Fig. 4). In 2-year-old adult abalones, *Ht-Lus* is expressed in the shell-forming tissue (Fig. 4).

3.3. Localisation of *Ht-Lus* expression in 7-day-old juvenile

Following metamorphosis, the juvenile shell is elaborated from the edge of the protoconch. This post-metamorphosis shell material can

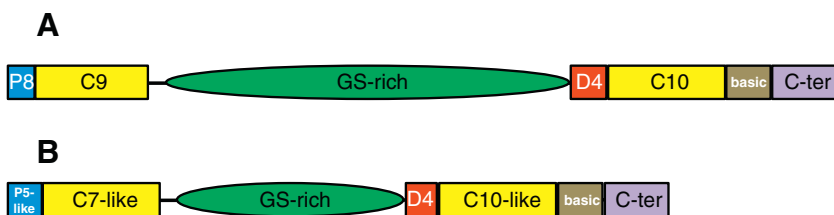


Fig. 2. Comparison of partial Lustrin A modular structure from *Haliotis rufescens* (A) and *Haliotis tuberculata* (B). This region of *Ht-Lus* is 124 residues shorter than the corresponding region in *Hruf-Lus* primarily because of the shorter GS-rich domain. The Pro-rich domain in *Ht-Lus* shares more identity with *Hruf-P5* than with *Hruf-P8*, and the first Cys-rich domain in *Ht-Lus* shares more identity with *Hruf-C7* than *Hruf-C9*. P: Pro-rich domain; C: Cys-rich domain; GS-rich: Gly-Ser-rich domain; D4: Asp-rich domain; C-ter: C-terminus (WAP).



**Fig. 3.** A representative northern blot against *H. tuberculata* *Lustrin A* from total mantle RNA. Two closely spaced bands are visible with calculated molecular weights of approximately 6.4 kb and 6.0 kb.

be easily distinguished from the larval shell as it is highly textured relative to the protoconch (“js” in Fig. 5). At this stage, when the animal is retracted into the shell, the mantle covers the head and is visible under the junction between the protoconch and the juvenile shell (“m” in Fig. 5A). Whole mount in situ hybridisation (WMISH) was used to localise cells expressing *Ht-Lus* in post-larvae and juveniles. In 7-day-old post-larvae, a strong *Ht-Lus* signal was detected at the mantle edge (Fig. 5B). A lateral anterior view illustrates *Ht-Lus* positive cells all along the mantle edge (Fig. 5C), while a dorsal view indicates that *Ht-Lus* transcripts are located throughout the entire whole cell cytoplasm (Fig. 5D). Although the signal was exclusively restricted to the mantle edge, not all mantle edge cells were *Ht-Lus* positive (Fig. 5D). In a few animals, a weak signal could also be observed in the visceral mass or in the foot (Fig. 5B, C). However this signal was also observed in

negative controls, and we consider this to be a non-specific background (data not shown).

### 3.4. Localisation of *Ht-Lus* expression in 2-month-old juvenile

In 2-month-old abalones, the juvenile shell is well developed and displays the typical flattened shape of the adult shell. A light brown background colour is present with darker brown stripes running in the same direction as the direction of shell growth. The protoconch is also still visible (“p” in Fig. 6A). Removing the shell and periostracum reveals the underlying mantle which covers the dorsal surface of the animal (Fig. 6B). WMISH against *Ht-Lus* reveals a strong signal all along the mantle edge (Fig. 6B). An enlargement of the mantle edge in dorsal view (Fig. 6D) showed that the signal is restricted to the cytoplasm of a single row of cells with the nucleus of these cells clearly located in a basal position, a characteristic of cells engaged in an extensive secretory activity (Fig. 6D). In this animal, all mantle edge cells were not *Ht-Lus* positive, similar to the pattern observed in 7-day-old post-larvae (Fig. 6C, D cf. Fig. 5C, D). In a slightly larger 2-month-old individual, all mantle edge cells were *Ht-Lus* positive (Fig. 6E). In this larger animal, the nacre forming region, a more proximal region of the mantle, was also *Ht-Lus* positive (Fig. 6F).

## 4. Discussion

Abalone nacre is a highly organized and fracture resistant microstructure produced by a specific combination of matrix proteins which constitute less than 5% of the shell weight (Currey, 1977; Jackson et al., 1988). In *H. tuberculata*, the early protoconch was shown to be mostly composed of amorphous CaCO<sub>3</sub> while veliger stages showed a gradually aragonitic crystallisation (Gaume et al., 2011). SEM examination of juvenile shell cross-sections evidenced a post-metamorphic transition in crystalline microstructure with mineral ordering in tablets within the inner layer (Auzoux-Bordenave et al., 2010). The cell types and secreted proteins involved in the ontogeny of these shell microstructures must be identified and characterised to fully understand the process of molluscan biomineralisation. In this study, we have isolated and characterised a partial fragment of a *Lustrin A* ortholog in the European abalone *H. tuberculata*. *Lustrin A* was the first nacreous protein to be identified in any *Haliotis* species (Shen et al., 1997). In *H. rufescens* *Lustrin A* is a large multi-domain protein, encoded by 4.7 and/or 5.5 kb transcripts thought to possess multiple functions (Shen et al., 1997). In *H. tuberculata*

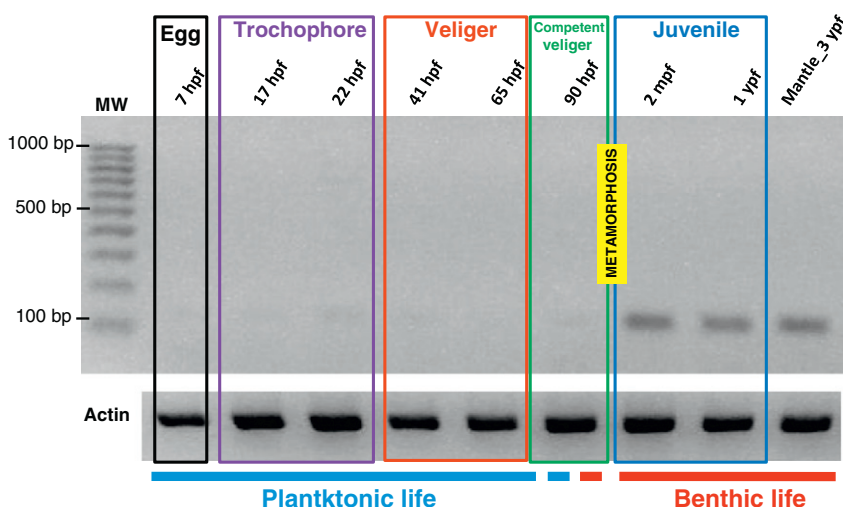


**Fig. 4.** Relative expression levels of *Ht-Lus* throughout the development of *H. tuberculata*. Actin was used as a control to ensure equal cDNA synthesis efficiency and template loading into the RT-PCR reactions. Coloured rectangles indicate distinct developmental stages. Egg (7 hpf), trochophore (17 and 22 hpf) and veliger (41 and 65 hpf) stages correspond to planktonic stages. Competent veliger larvae (90 hpf) begin to settle and explore benthic substrates. Juveniles (2 mpf and 1 ypf) and adults (3 ypf) are strictly benthic. Total RNA was extracted from whole animals for egg, larvae and juveniles. For adults (3 ypf), total RNA was extracted from the mantle tissue of 3-year-old abalones. Abbreviations: hours post-fertilisation (hpf), months post fertilisation (mpf), years post-fertilisation (ypf).

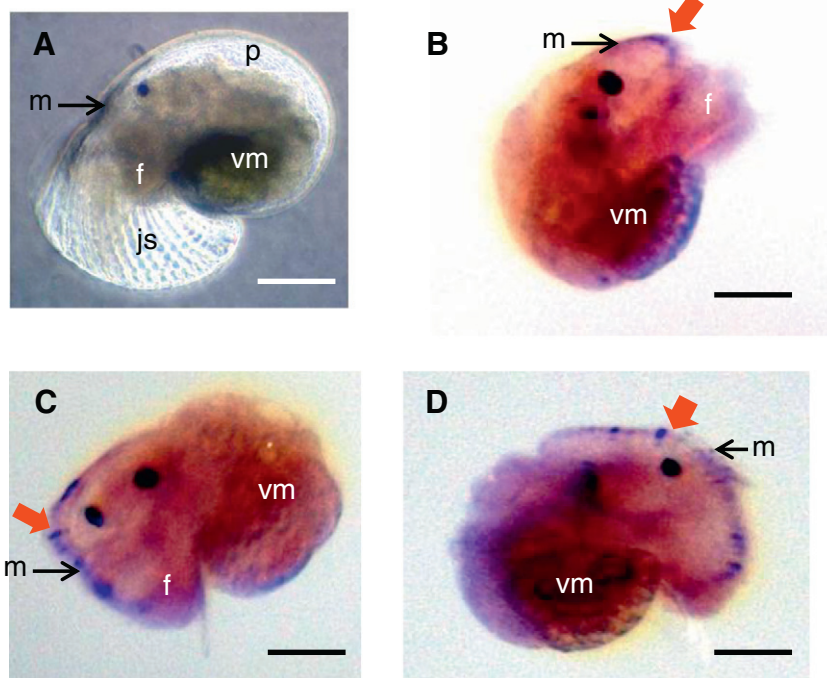


**Fig. 5.** Localisation of *Ht-Lus* expression in 7 day-old juvenile *H. tuberculata*. (A) 7-day-old abalone observed by phase contract microscopy. The larval protoconch (p) and the forming juvenile shell (js) are easily distinguished. (B–D) *Ht-Lus* expression revealed by whole mount in situ hybridisation in 7-day-old decalcified juveniles. *Ht-Lus* expression is restricted to the mantle edge (purple signal indicated by red arrows). (A) Left profile view, (B) right profile view (C) lateral-anterior view, and (D) dorsal view with the mantle covering the whole head of the abalone. Abbreviations: visceral mass (vm), mantle (m), foot (f). Scale bar = 100 µm.

there also appears to be two *Lustrin* transcripts, with estimated sizes of 6.0 and 6.4 kb (Fig. 3). The repetitive nature of this gene makes it extremely challenging to clone in its entirety, and further experiments will be necessary to obtain the full length of the different cDNAs which could be characterised by variable Proline and Cysteine rich domain numbers.

The deduced amino acid sequence of the *Ht-Lus* fragment we have isolated displays a modular structure consisting in (i) one short Pro-rich domain, (ii) two highly conserved Cys-rich domains, (iii) a Gly-Ser-rich domain, (iv) a basic domain, and (v) a C-terminus domain with homology to Whey Acidic Protein (WAP). These domains possess high similarity with those of *Lustrin A* from *H. rufescens*. Although the modular structure of *Lustrin A* is conserved there are notable differences. For example, the Gly-Ser-rich domain in *Ht-Lus* is 119 residues shorter than that in *H. rufescens* *Lustrin A*, while the basic domain of *Ht-Lus* consists of 40% basic residues, giving this region a higher predicted pI than that in *H. rufescens*. The net positive charge of the basic domain at pH 7.4 is suggested to allow it to interact with carbonate ions ( $\text{CO}_3^{2-}$ ) and/or with polyanionic molecules such as acidic proteins which are major components of the soluble organic matrix (Shen et al., 1997). The Pro-, Cys- and Gly-Ser-rich domains of *Hruf-Lust* were suggested to contribute to the flexibility of the protein (Shen et al., 1997). Cys-rich domains were also shown to adopt a loop conformation at pH 7.4, the pH in which the organic matrix assembles (Zhang et al., 2002). The C-terminal domain which exhibits homology to WAPs contains a characteristic eight cysteine motif forming the “four-disulphide core” (Ranganathan et al., 1999). The WAP domain is highly evolutionarily conserved and is found in many metazoan lineages such as mammals, birds, reptiles, amphibians, fish and invertebrates (Smith, 2011). This domain is suggested to act as an active protease inhibitor (Treccani et al., 2006).

Our RT-PCR results revealed an expression of *Ht-Lus* only after metamorphosis. In *H. tuberculata*, aragonitic tablets of nacre were first observed in 2-month-old juveniles (Auzoux-Bordenave et al., 2010).

*Ht-Lus* expression according to our RT-PCR results is therefore broadly correlated with the ontogenetic onset of nacre deposition. Our whole mount in situ hybridisation results also give us further insight into the expression and function of *Ht-Lus*. *Ht-Lus* transcripts were detected in 7-day-old post-larvae, specifically in the distal edge of the mantle. At this early-metamorphic stage, the juvenile shell begins to acquire its flattened morphology with its characteristic texture and pigmentation. The microstructure of the post-metamorphic revealed two poorly defined prismatic layers with a granular layer in between (Auzoux-Bordenave et al., 2010). No organized nacre is present at this stage and the shell only contains aragonite. If we assume that *Ht-Lus* transcripts also indicate the presence of functional *Ht-Lus* protein, then there appears to be a discrepancy of at least 7 weeks between the onset of *Ht-Lus* expression and nacre deposition. This discrepancy could be accounted for in several ways. First, *Lustrin A* is unlikely to be the only protein required for nacre deposition, perhaps the full complement of nacre forming proteins and other organic molecules is not secreted by the mantle of 7-day old larvae. Second, a critical concentration of *Lustrin A* protein may be required before crystals of nacre can be deposited. The few *Lustrin A* positive cells in the early post-larvae may not be sufficient to drive this crystallisation. A third possibility, and our favoured interpretation, is that *Lustrin A* may have multiple functions, and the expression domain observed in the distal edge of the mantle may not be responsible for nacre deposition at this stage.

In 2-month-old juveniles, *Ht-Lus* continues to be expressed in the distal edge of the mantle as it is in 7-day old larvae. Furthermore, the largest individuals also express *Ht-Lus* in an additional broad proximal region of the mantle (Fig. 6F). In individuals of this age the mantle is more differentiated than in younger individuals, and a regionalization of cells similar to that of the adult mantle can be observed in *H. asinina* and *H. tuberculata* (Sud et al., 2002; McDougall et al., 2011). The expression of *Ht-Lus* in two distinct zones (the distal edge and the broad proximal region) and in a temporally disconnected manner, suggests that these two domains fulfil different functions. Furthermore, the fact that

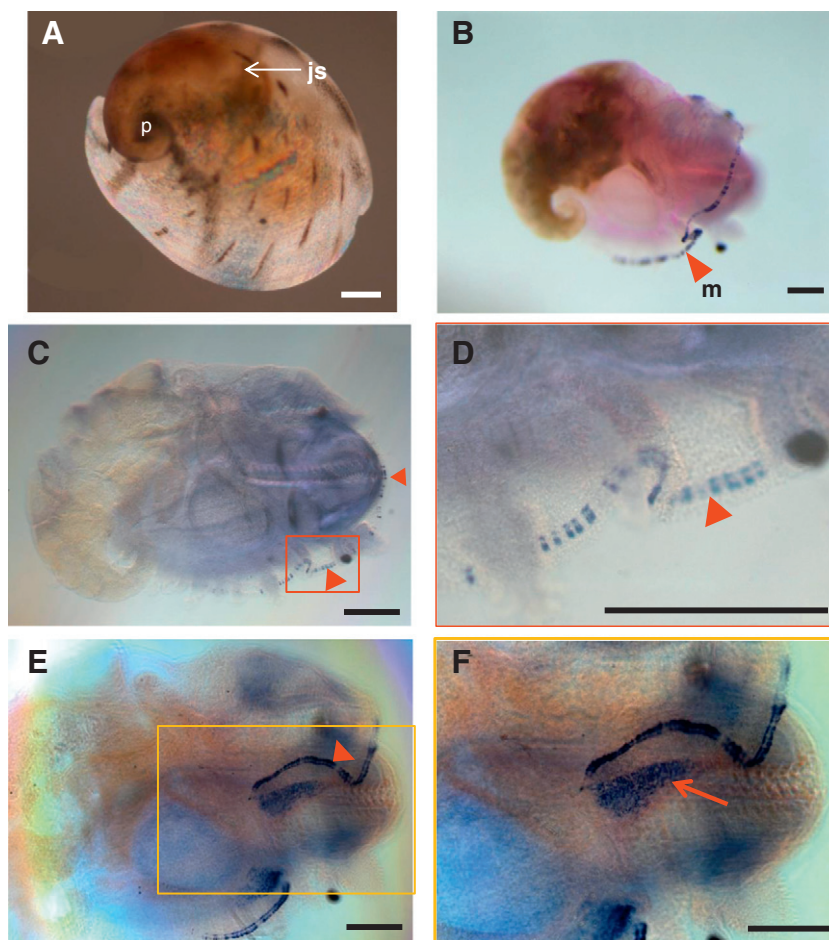


**Fig. 6.** Localisation of *Ht-Lus* gene expression in 2-month-old *H. tuberculata*. (A) 2-month-old abalone observed by light microscopy revealing the ornamented, flattened juvenile shell (js) which is easily distinguished from the larval protoconch (p). (B–F) Localisation of *Ht-Lus* expression by whole mount in situ hybridisation in 2-month-old decalcified juvenile. (B) Dorsal view. *Ht-Lus* is expressed all along the mantle edge (arrow head). (C) Ventral view. (D) A magnified view of the boxed region in (C) shows that some cells do not express *Ht-Lus*. The basal position of the nucleus in *Ht-Lus* positive cells is also visible in this image. (E) Dorsal view of a larger 2-month-old individual than that in (C). *Ht-Lus* in this animal is localised in the mantle edge and also in the putative nacre-forming region (white arrows). The left mantle lobe is folded back on itself in this sample such that the edge of the mantle appears to be posterior to the nacre-forming region. (F) Magnified view of the boxed region in E. Scale-bar = 200  $\mu\text{m}$ .

there are apparently two distinct *Ht-Lus* transcripts (as suggested by the northern blot results; Fig. 3) raises the possibility that these two spatial expression domains in the mantle actually may represent the two different transcripts. In the only other study to investigate the spatial and/or temporal expression of *Lustrin A*, Jackson et al. (2007) reported a distal expression domain in 1 mm *H. asinina* juveniles, but no expression was detected in the distal edge of the mantle. We suggest that it is the distal expression domain that is associated with nacre deposition, while the expression in the mantle edge has an as yet unidentified function.

Since the identification of *Lustrin A* in *H. rufescens* (Shen et al., 1997), there have been several investigations into the role of this unique multi-domain shell matrix protein. The main functions attributed to *Lustrin A* are (i) inter-nacre tablet adhesion, (ii) elastomeric properties that contribute to shell fracture resistance, (iii) protease inhibition, and (iv) binding of acidic shell-matrix proteins. The ability of *Lustrin A* to adhere to calcium was shown to be played by both the “D4” peptide located just downstream of the glycine-serine-rich domain (Wustman et al., 2003), and the WAP domain which adheres to crystals in vitro (Treccani et al., 2006). AFM experiments suggest that it is the *Lustrin*-containing adhesive organic polymer found between the tablets of nacre that are responsible for the sawtooth-like force-extension curves observed in nacre under stress (Smith et al., 1999). This elastomeric property has been suggested to be conferred by the glycine-serine rich domain (Shen et al., 1997) and inter-molecular disulphide bonds

formed between the Cys-rich domains (Zhang et al., 2002). *Lustrin A* also has the capacity to interact with acidic shell matrix proteins through its basic domain (Shen et al., 1997). Acidic matrix proteins such as AP7 and AP24 are an abundant and diverse component of the organic shell matrix, and they are known to influence calcification in vitro (Michenfelder et al., 2003). Another important role of *Lustrin A* could be its capacity to bind proteases through the WAP domain (Shen et al., 1997). Such a property would protect the organic component of the shell from degradation through the action of proteases secreted by shell-boring predators.

This diverse repertoire of functions places the *Lustrin A* protein into a special category of the shell forming secretome. Here, we demonstrate that in addition to its diverse functional roles, *Lustrin A* also has multiple spatial expression domains within the mantle of developing post-larvae. We suggest that *H. tuberculata* *Lustrin A* is either conferring all of these diverse properties to different layers of the post-larval and juvenile shells, or *Lustrin A* is imparting different properties to different shell layers. Because we have not isolated the full length sequences of the two transcripts we observe in adult mantle tissue (Figs. 3 and 6), we cannot determine whether the two expression domains we observe by WMISH are generated by the two distinct transcripts or not. Such information would afford us further insight into the mechanism of action of this fascinating shell forming protein. Nonetheless, our data does clearly demonstrate that there is a complex ontogenetic component to shell formation that is currently under appreciated. Efforts aimed at

the synthetic production of biomaterials such as molluscan shells would be well informed by such observations.

## Acknowledgements

This work was financed in part by the ATM program “Biomineralisation” of the MNHN funded by the Ministère délégué à l'Enseignement Supérieur et à la Recherche (Paris, France). This work was supported by the Deutsche Forschungsgemeinschaft (DFG) funding to DJJ through the CRC for Geobiology and the German Excellence Initiative.

## References

- Addadi, L., Weiner, S., 1985. Interactions between acidic proteins and crystals: stereochemical requirements in biomineralisation. *Proc. Natl. Acad. Sci. U. S. A.* 82, 4110–4114.
- Addadi, L., Raz, S., Weiner, S., 2003. Taking advantage of disorder: amorphous calcium carbonate and its roles in biomineralisation. *Adv. Mater.* 15, 959–970.
- Amos, F.F., Evans, J.S., 2009. AP7, a partially disordered pseudo C-RING protein, is capable of forming stabilized aragonite *in vitro*. *Biochemistry* 48, 1332–1339.
- Auzoux-Bordenave, S., Badou, A., Gaume, B., Berland, S., Helléouet, M.-N., Milet, C., Huchette, S., 2010. Ultrastructure, chemistry and mineralogy of the growing shell of the European abalone *Haliotis tuberculata*. *J. Struct. Biol.* 171, 277–290.
- Bédouet, L., Marie, A., Berland, S., Marie, B., Auzoux-Bordenave, S., Marin, F., Milet, C., 2012. Proteomic strategy for identifying mollusc shell proteins using mild chemical degradation and trypsin digestion of insoluble organic shell matrix: a pilot study on *Haliotis tuberculata*. *Mar. Biotechnol.* 14, 446–458.
- Blank, S., Arnoldi, M., Khoshnavaz, S., Treccani, L., Kuntz, M., Mann, K., Grathwohl, G., Fritz, M., 2003. The nacre protein perlucin nucleates growth of calcium carbonate crystals. *J. Microsc.* 212, 280–291.
- Courtois de Viçosa, G., Viera, M.P., Bilbao, A., Izquierdo, M.S., 2007. Embryonic and larval development of *Haliotis tuberculata coccinea* Reeve: an indexed micro-photographic sequence. *J. Shellfish Res.* 26, 847–854.
- Currey, J.D., 1977. Mechanical properties of mother of pearl in tension. *Proc. R. Soc. B Biol. Sci.* 196, 443–463.
- Falini, G., Albeck, S., Weiner, S., Addadi, L., 1996. Control of aragonite or calcite polymorphism by mollusc shell macromolecules. *Science* 271, 67–69.
- Gaume, B., Fouchereau-Peron, M., Badou, A., Helléouet, M.-N., Huchette, S., Auzoux-Bordenave, S., 2011. Biomineralisation markers during early shell formation in the European abalone *Haliotis tuberculata*. *Linnaeus. Mar. Biol.* 158, 341–353.
- Giusti, A.F., Hinman, V.F., Degnan, S.M., Degnan, B.M., Morse, D.E., 2000. Expression of a *Scr/Hox5* gene in the larval central nervous system of the gastropod *Haliotis*, a non-segmented spiralian lophotrochozoan. *Evol. Dev.* 2, 294–302.
- Jackson, A.P., Vincent, J.F.V., Turner, R.M., 1988. The mechanical design of nacre. *Proc. R. Soc. B Biol. Sci.* 234, 415–440.
- Jackson, D., McDougall, C., Green, K., Simpson, F., Worheide, G., Degnan, B., 2006. A rapidly evolving secretome builds and patterns a sea shell. *BMC Biol.* 4, 40.
- Jackson, D., Worheide, G., Degnan, B., 2007. Dynamic expression of ancient and novel molluscan shell genes during ecological transitions. *BMC Evol. Biol.* 7, 160.
- Jardillier, E., Rousseau, M., Gendron-Badou, A., Fröhlich, F., Smith, D., Martin, M., Helléouet, M.-N., Huchette, S., Doumenc, D., Auzoux-Bordenave, S., 2008. A morphological and structural study of the larval shell from the abalone *Haliotis tuberculata*. *Mar. Biol.* 154, 735–744.
- Joubert, C., Piquemal, D., Marie, B., Manchon, L., Pierrat, F., Zanella-Cleon, I., Cochenec-Laureau, N., Gueguen, Y., Montagnani, C., 2010. Transcriptome and proteome analysis of *Pinctada margaritifera* calcifying mantle and shell: focus on biomineralisation. *BMC Genomics* 11, 613.
- Le Roy, N., Marie, B., Gaume, B., Guichard, N., Delgado, S., Zanella-Cleon, I., Becchis, M., Auzoux-Bordenave, S., Sire, J.-Y., Marin, F., 2012. Identification of two carbonic anhydrases in the mantle of the European abalone *Haliotis tuberculata* (Gastropoda, Haliotidae): phylogenetic implications. *J. Exp. Zool. B* 318, 353–367.
- Lowenstam, H.A., Weiner, S., 1989. *On Biomineralisation*. Oxford University Press, New York-Oxford.
- Mann, S., 2001. *Biomineralisation. Principles and Concepts in Bioinorganic Materials Chemistry*. Oxford University Press, Oxford.
- Mann, K., Siedler, F., Treccani, L., Heinemann, F., Fritz, M., 2007. Perlinhibin, a cysteine-, histidine-, and arginine-rich mini-protein from abalone (*Haliotis laevigata*) nacre, inhibits *in vitro* calcium carbonate crystallization. *Biophys. J.* 93, 1246–1254.
- Marie, B., Marie, A., Jackson, D.J., Dubost, L., Degnan, B.M., Milet, C., Marin, F., 2010. Proteomic analysis of the organic matrix of the abalone *Haliotis asinina* calcified shell. *Proteome Sci.* 8.
- Marin, F., Luquet, G., Marie, B., Medakovic, D., 2008. Molluscan shell proteins: primary structure, origin, and evolution. *Curr. Top. Dev. Biol.* 80, 209–276.
- McDougall, C., Green, K., Jackson, D.J., Degnan, B.M., 2011. Ultrastructure of the mantle of the gastropod *Haliotis asinina* and mechanisms of shell regionalization. *Cells Tissues Organs* 194, 103–107.
- Michenfelder, M., Fu, G., Lawrence, C., Weaver, J.C., Wustman, B.A., Taranto, L., Evans, J.S., Morse, D.E., 2003. Characterization of two molluscan crystal-modulating biomineralisation proteins and identification of putative mineral binding domains. *Biopolymers* 70, 522–533.
- Ranganathan, S., Simpson, K.J., Shaw, D.C., Nicholas, K.R., 1999. The whey acidic protein family: a new signature motif and three-dimensional structure by comparative modeling. *J. Mol. Graph. Model.* 17, 106–113.
- Shen, X., Belcher, A.M., Hansma, P.K., Stucky, G.D., Morse, D.E., 1997. Molecular cloning and characterization of Lustrin A, a matrix protein from shell and pearl nacre of *Haliotis rufescens*. *J. Biol. Chem.* 272, 32472–32481.
- Smith, V.J., 2011. Phylogeny of whey acidic protein (WAP) four-disulfide core proteins and their role in lower vertebrates and invertebrates. *Biochem. Soc. Trans.* 39, 1403–1408.
- Smith, B.L., Schaffer, T.E., Viani, M., Thompson, J.B., Frederick, N.A., Kindt, J., Belcher, A., Stucky, G.D., Morse, D.E., Hansma, P.K., 1999. Molecular mechanistic origin of the toughness of natural adhesives, fibres and composites. *Nature* 399, 761–763.
- Sud, D., Poncet, J.M., Saïhi, A., Lebel, J.-M., Doumenc, D., Boucaud-Camou, E., 2002. A cytological study of the mantle edge of *Haliotis tuberculata* L. (Mollusca, Gastropoda) in relation to shell structure. *J. Shellfish Res.* 21, 201–210.
- Treccani, L., Mann, K., Heinemann, F., Fritz, M., 2006. Perlwapin, an abalone nacre protein with three four-disulfide core (whey acidic protein) domains, inhibits the growth of calcium carbonate crystals. *Biophys. J.* 91, 2601–2608.
- Weiner, S., Dove, P.M., 2003. An overview of biomineralisation processes and the problem of the vital effect. *Rev. Mineral. Geochem.* 54, 1–29.
- Weiss, I.M., Kaufmann, S., Mann, K., Fritz, M., 2000. Purification and characterization of perlucin and perlustrin, two new proteins from the shell of the mollusc *Haliotis laevigata*. *Biochem. Biophys. Res. Commun.* 267, 17–21.
- Wustman, B.A., Weaver, J.C., Morse, D.E., Evans, J.S., 2003. Structure-function studies of the Lustrin A polyelectrolyte domains, RKSY and D4. *Connect. Tissue Res.* 44, 10–15.
- Wustman, B.A., Morse, D.E., Evans, J.S., 2004. Structural characterization of the N-terminal mineral modification domains from the molluscan crystal-modulating biomineralisation proteins, AP7 and AP24. *Biopolymers* 74, 363–376.
- Zhang, B., Wustman, B.A., Morse, D., Evans, J.S., 2002. Model peptide studies of sequence regions in the elastomeric biomineralisation protein, Lustrin A. I. The C-domain consensus-PG-, -NVNCT-motif. *Biopolymers* 63, 358–369.